Title

Discovery of genomic loci of the human cerebral cortex using genetically informed brain atlases

Journal

Science, 375(6580)

ISSN

0036-8075

Authors

Makowski, Carolina
van der Meer, Dennis
Dong, Weixiu
et al.

Publication Date

2022-02-04

DOI

10.1126/science.abe8457

Peer reviewed

HHS Public Access

Author manuscript

Science. Author manuscript; available in PMC 2022 September 13.

Published in final edited form as:

Science. 2022 February 04; 375(6580): 522–528. doi:10.1126/science.abe8457.

Discovery of genomic loci of the human cerebral cortex using genetically informed brain atlases*

Carolina Makowski[1], **Dennis van der Meer**[2,3], **Weixiu Dong**[4], **Hao Wang**[1], **Yan Wu**[4], **Jingjing Zou**[5], **Cin Liu**[1], **Sara B. Rosenthal**[6], **Donald J. Hagler Jr.**[1], **Chun Chieh Fan**[1], **William S. Kremen**[7], **Ole A. Andreassen**[2], **Terry L. Jernigan**[8], **Anders M. Dale**[1], **Kun Zhang**[4], **Peter M. Visscher**[9], **Jian Yang**[9,10], **Chi-Hua Chen**[1,†]

[1]Center for Multimodal Imaging and Genetics, University of California San Diego

[2]NORMENT Centre, Division of Mental Health and Addiction, Oslo University Hospital & Institute of Clinical Medicine, University of Oslo, Norway

[3]School of Mental Health and Neuroscience, Faculty of Health, Medicine and Life Sciences, Maastricht University, Maastricht, The Netherlands

[4]Department of Bioengineering, University of California San Diego

[5]Division of Biostatistics, Herbert Wertheim School of Public Health and Human Longevity Science, University of California San Diego

[6]Center for Computational Biology & Bioinformatics, University of California San Diego

[7]Department of Psychiatry and Center for Behavior Genetics of Aging, University of California San Diego

[8]Center for Human Development, University of California San Diego

[9]Institute for Molecular Bioscience, The University of Queensland, Brisbane, Queensland 4072, Australia

[10]School of Life Sciences, Westlake University, Hangzhou, Zhejiang 310024, China

Abstract

To determine the impact of genetic variants on the brain, we used genetically-informed brain atlases in genome-wide association studies of regional cortical surface area and thickness in

---

*This manuscript has been accepted for publication in *Science*. This version has not undergone final editing. Please refer to the complete version of record at http://www.sciencemag.org/. The manuscript may not be reproduced or used in any manner that does not fall within the fair use provisions of the Copyright Act without the prior, written permission of AAAS.

†Correspondence to: chc101@ucsd.edu (C.H.C.).

Author contributions: Study design: C.M., D.vd.M., W.D., H.W., Y.W., K.Z., P.M.V., J.Y., C.H.C; Data analysis: C.M., D.vd.M., W.D., Y.W., J.Z., H.W., S.B.R., C.H.C.; Manuscript writing: C.M., D.vd.M., W.D., C.H.C.; UKB data: D.vd.M., O.A.A., ABCD data: C.M., D.H., C.C.F., T.L.J., A.M.D.; single-cell data: W.D., Y.W., K.Z.; Data visualization: C.M., D.vd.M., W.D., Y.W., C.L., C.H.C.; Manuscript preparation and revisions: all authors.

Competing interests: Dr. Andreassen has received speaker's honorarium from Lundbeck and Sunovion, and is a consultant to HealthLytix. Dr. Dale is a Founder of and holds equity in CorTechs Labs, Inc, and serves on its Scientific Advisory Board. He is a member of the Scientific Advisory Board of Human Longevity, Inc. and receives funding through research agreements with General Electric Healthcare and Medtronic, Inc. The terms of these arrangements have been reviewed and approved by UCSD in accordance with its conflict of interest policies. The other authors declare no competing interests.

39,898 adults and 9136 children. We uncovered 440 genome-wide significant loci in the discovery cohort and 800 from a post-hoc combined meta-analysis. Loci in adulthood were largely captured in childhood, showing signatures of negative selection, and were linked to early neurodevelopment and pathways associated with neuropsychiatric risk. Opposing gradations of decreased surface area and increased thickness were associated with common inversion polymorphisms. Inferior frontal regions, encompassing Broca's area which is important for speech, were enriched for human-specific genomic elements. Thus a mixed genetic landscape of conserved and human-specific features is concordant with brain hierarchy and morphogenetic gradients.

One Sentence Summary:

Genetically-informed brain atlases discover novel genomic loci of neurodevelopmental patterning in adult and youth cortex.

Large-scale magnetic resonance imaging (MRI) and genetics datasets have afforded the opportunity to discover common genetic variants contributing to the morphology of the human cortex. Studies in model organisms have revealed intricate genetic mechanisms underlying cortical area and thickness/laminar patterning, although it has been challenging to define aspects of cortical development that are shared across mammals compared to those that are human-specific (1). Nevertheless, many studies have shown support for the radial unit hypothesis that posits differential neurodevelopment programs shaping and regulating these two cortical measures (2).

Consistent with this, the ENIGMA consortium's genome-wide association study (GWAS) of the human cortex found many variants associated with surface area and thickness linked to neurodevelopmental processes during fetal development (3). Such evidence for neurodevelopmental programming indicates the need to investigate these questions at earlier ages, as previous cortical GWAS have almost exclusively been conducted in older adults.

Cortical expansion and regional patterning are largely genetically determined (2); thus we used data-driven genetically-informed atlases in the current study (4, 5), in contrast to atlases primarily determined by sulcal-gyral patterns. These genetically-determined atlases capture patterns of hierarchical genetic similarity following known developmental gradients which shape the cortex along their anterior-posterior (A-P) and dorsal-ventral (D-V) axes, including 12 surface area and 12 thickness regions (2, 4, 5), and increase discoverability of genetic variants underlying the cortex (6).

Results

Genetic variants underlying cortical thickness and area

In our discovery UK Biobank (UKB) sample of 32,488 individuals (Table S1), we found 440 genome-wide significant (mixed linear model association tests (7), $p<5e-8$) variants after clumping each phenotype separately in PLINK (8) ($r^2=0.1$, 250kb), where 305 and 88 regional genetic variants were associated with the 12 surface area and 12 cortical thickness phenotypes, respectively (Fig.1; Tables S2-3). Twenty-seven genetic variants were significantly associated with total surface area and 20 variants with mean cortical thickness

(Table S2). After correction for multiple comparisons, 234 genetic variants remained significant (p<2.27e-9, 5e-8/t_e, with t_e=22 being the effective number of independent traits). We performed subsequent functional analyses for the 393 regional variants. Single nucleotide polymorphisms (SNPs) were mapped to genes on the basis of their genomic position with FUMA (9). Across all phenotypes, SNPs were significantly enriched for non-coding regions (Fig.1; Table S4; 44.0% enriched for intronic variants, 33.4% intergenic, and 17.7% non-coding intronic RNA, Fisher's exact test P<0.05).

Replication & Generalization

Replication was performed on an admixed sample of 7410 individuals from UKB including 2232 of European descent using Mixed Linear Model Association (MLMA) analysis in GCTA (10). We modeled population structure using GENESIS (11) to estimate principal components and kinship. Estimated genetic effects in the discovery dataset were correlated with those in the replication dataset, as indexed by significant beta correlations (ranging from r=0.66–0.95 after correcting for errors in the estimated SNP effects) (Fig. S1), sign concordance rate (binomial test, p<0.05), and proportion of variants replicated after multiple comparison correction (12).

MLMA and GENESIS were also used for generalization to data from the Adolescent Brain Cognitive Development (ABCD) Study® (N=9136) (Table S1), given the high degree of admixture and relatedness in this sample. Generalization to ABCD was quite high, as can be observed through significant beta correlations (r range 0.46–0.92) (Fig S2), sign concordance rate, and proportion of variants replicated after correction for multiple comparisons (12). This suggests that the genetic architecture of the cortex found in adulthood is largely generalizable to earlier life stages of neurodevelopment, particularly for surface area. We also examined correspondence between the two datasets by calculating genetic correlations with Linkage Disequilibrium (LD) SCore regression (LDSC) for each region. Eighteen of 24 phenotypes were significantly genetically similar between ABCD and UKB (r_g range 0.38–1.21) (Fig S3).

Given the evidence of comparable results, we ran a joint meta-analysis of the three samples using METAL (12). After clumping each phenotype separately to obtain independent loci, the meta-analysis revealed 800 genome-wide significant regional loci with 467 passing correction for multiple comparisons (Table S5). Of 800 loci, 526 were found to be independent by merging hits from these 26 phenotypes into one file and clumping with PLINK (8) (r^2=0.1, 250kb). With the exception of one SNP, all had a non-significant heterogeneity p-value (p>1e-6) associated with Cochran's Q statistic, suggesting comparability among samples. SNPs from the meta-analysis with a significant heterogeneity p-value<1e-6 are in Table S6.

Comparison to previous cortical GWAS

We used conditional and joint analysis (COJO) (13) to identify novel loci compared to the most recent GWAS of cortical architecture which identified 369 loci (3). Of these loci, 206 were found to be independent by clumping all 70 phenotypes together (r^2=0.1, 250kb).

COJO revealed that 63.6% of our 393 regional variants remained genome-wide significant and thus are considered as novel associated variants (12) (Table S7).

Assigning SNPs to genes and neuropsychiatric implications

All SNPs in LD (r^2>0.6) with the 393 regional variants were mapped to genes using positional, gene expression (eQTL), and chromatin interaction information in FUMA SNP2GENE (9). This mapped our genetic variants to 915 genes (Tables S8-9). MAGMA gene-based analyses yielded 575 significant genes (mean χ^2 statistics, p<2.6e-6) (Table S10). Many significant genes are related to neurodevelopmental disorders (autism, epilepsy, microcephaly) or dementia according to the NIH Genetics Home reference (Table S11).

Further support for this conclusion was determined by investigating the shared genetic effects between our brain phenotypes and disorders by estimating genetic correlations through LDSC (Fig S4; Table S12). We found a significant association between global surface area and ADHD after multiple comparison correction, as well as nominal significant associations (e.g. temporal area with schizophrenia and autism spectrum disorder (ASD)). To examine putative causal association, we performed Mendelian Randomization (14) on global area and ADHD that showed the most significant Rg, and did not find evidence of causality. We also examined ASD, a neurodevelopmental disorder with early onset, and its relationship with anteromedial temporal area indexed by a significant Rg. We found a significant unidirectional causation (b_{xy}=−0.36, p =9.5e-05), indicating that decreased anteromedial temporal area may cause ASD. These SNPs could be missed in classical GWAS of ASD, but nevertheless are important genetic factors in the pathogenesis of this disorder through their contributions to anteromedial temporal morphology.

Genetic architecture of cortex

Compared to other common complex traits, cortical phenotypes tend to have low polygenicity (proportion of genome-wide SNPs with non-null effects; range: 0.0038–0.040; area: $\bar{p}$ =0.0085± 0.0011; thickness: $\bar{p}$ =0.015±0.0039) and average to high SNP-based heritability (range: 0.14–0.37; area: $\overline{h^2}$=0.27±0.012; thickness: $\overline{h^2}$=0.20±0.011) (Fig.2). Pedigree-based heritability for the UKB discovery sample (range: 0.31–0.95), calculated with multiple genetic relatedness matrices (GRMs) (15), and twin-based heritability approximated by Falconer's formula from the ABCD sample (range: 0.39–0.96) can be found in Table S13. Negative selection signatures can be inferred by the relationship between minor allele frequency and effect size, quantified by the S parameter implemented in SBayesS (16) (Fig S5). We found that loci associated with our cortical phenotypes may be under strong negative selection pressures (16) compared to phenotypes with similar levels of heritability and polygenicity (range: −0.99–0.045; area: $\bar{S}$=−0.79±0.11; thickness: $\bar{S}$ =−0.72±0.18). It should be noted that π is slightly dependent on sample size and thus should be interpreted with caution. However, others have shown similar estimates of polygenicity for brain phenotypes (17).

Partitioned heritability

Different functional regions of the genome can contribute disproportionately to complex human traits. Thus, we applied stratified LDSC regression to partition heritability estimates of our 24 cortical phenotypes for 97 annotations from the baseline model (18, 19) (Table S14), from which we focused on enriched annotations where regression coefficients are significantly positive ($z>1.96$, two-tailed $p<0.05$). We classified the annotations into three categories determined from conserved, developmental, and regulatory genomic partitions. We found seven conserved annotations (found in primates and other mammals) to be significantly enriched after multiple comparison correction ($p<0.0025$, where $p< 0.05/t_e$, Figure 3A, Table S15) across 16 cortical phenotypes, with notable enrichment for seven phylogenetically conserved cortical regions (e.g. medial temporal lobe, motor and orbitofrontal regions) for the annotation “ancient sequence age human promoter”. This conserved promoter annotation reflects a genomic region that is evidenced to have existed prior to the evolutionary split of marsupial and placental mammals (18).

Seven regions, mostly indexing surface area, were significantly enriched for developmental annotations of fetal DNAse I hypersensitive sites (DHSs), a marker of accessible chromatin (20), along with enrichment of 15 cortical phenotypes for 13 regulatory annotations (Table S15). An additional partitioned heritability analysis with differential methylation regions (DMRs) associated with present-day humans was compared to Neanderthal and Denisovan genomes (21). Conditional on the baseline model, perisylvian thickness was nominally enriched for present-day human DMRs (LDSC Jackknife test, $p=0.03$). By partitioning the genome into meaningful functional categories, we capture patterns of hierarchical brain organization with evolutionarily conserved (paralimbic, sensory-motor) regions enriched for conserved and developmental annotations, and association areas more strongly associated with regulatory annotations.

Gene Ontology enrichment

To elucidate the biological pathways associated with our discovered genetic variants, MAGMA-mapped genes were input into MsigDB to obtain gene ontology (GO) terms. Twenty-six GO terms, predominantly related to neurodevelopment, were significantly associated with our brain phenotypes after Bonferroni correction (Fig.3B; Table S16). Notable biological pathways included *WNT*/beta-catenin, *TCF*, *FGF*, and hedgehog signaling, important for axis specification and areal identity (1). For higher-order association regions, the dorsolateral prefrontal cortex was linked to cortical tangential migration.

Three-dimensional genetic characterization of cortex.

To better understand the relationship between our cortical phenotypes, we computed phenotypic and genetic correlation matrices via LDSC (Fig.4A). Significant correspondence was observed between matrices (Mantel test: $r=0.85$, $p=0.001$), suggesting substantial genetic influences on cortical patterning. Hierarchical clustering was applied to genetic correlations of area and thickness separately, revealing a clear separation in genetic architecture between A-P divisions in area, and between D-V divisions in thickness (Figs.4A, 4B and S6). Regions anatomically closer to each other tended to be more

correlated with each other. However, homologous regions in contralateral hemispheres had high genetic correlations despite their physical distance (4) (Table S18).

Given the observed correlations, we sought to estimate the shared genetic effects across phenotypes with genomic Structural Equation Modeling (SEM) (Figs 4C, S7-8) (12, 22). We found two-factor models fit our data well (CFI >0.98). The two latent factors recapitulated the A-P and D-V gradations of cortical patterning for area and thickness, respectively. The strongest association signals between the latent factors and variants reside in the 17q21.31 inversion region for area (p<1.48e-56), and more diverse effects including chromosomes 3 and 17 for thickness (p <3.39e-15) (Fig.S8). We further performed association testing of inversion polymorphisms on 17q21.31 with our cortical phenotypes (Table S19). We found the inverted allele to be highly associated with overall surface area reductions, with stronger effects in posterior regions along the A-P gradient, and a modest positive correlation with increasing thickness in ventral regions. The opposing effects on area and thickness may in part account for the observation of a modest negative association between area and thickness ("cortical stretching") after accounting for total brain size (23).

After extracting salient latent factors underlying multiple brain regions, we searched for pleiotropic loci between pairs of regions. We used COJO to map SNPs with potential pleiotropic effects (e.g. that influence two regions), defined by the loci of region *i* that were no longer genome-wide significant when conditioned on the loci of region *k* (13). Using this approach, we found 107 of our 393 loci had pleiotropic effects on two phenotypes (Fig.4B, Table S20). Parietal and posterolateral temporal area shared 8 SNPs with antagonistic effects (i.e. increasing area of one region while decreasing area of the other); these regions show good correspondence between ABCD and UKB and are both enriched for fetal DNAse hypersensitive sites (Fig 3A). Two of these antagonistic SNPs, rs10878269 and rs142166430, are intronic variants of *MSRB3*, a gene important for protein repair and metabolism (24).

We also noted antagonistic pleiotropic effects of two SNPs (rs12676193 & rs6986885) in the 8p23.1 inversion polymorphism linked to decreases in motor premotor area and increases in perisylvian thickness (Table S19). These SNPs were mapped to *MSRA*, important for repair of oxidatively damaged proteins (25). Further, the 8p23.1 region is considered to be a potential hub for neurodevelopmental and psychiatric disorders (26). Another notable SNP with pleiotropic effects was rs888812 with antagonistic effects on precuneus and prefrontal area. This and other variants were mapped to *NR2F1/COUP-TF1*, a transcription factor influencing A-P patterning of the cortex in development (1).

Enrichment of cell type-specific accessible chromatin sites and fine-mapping to regulatory regions of genes

To map putative causal genes for our genetic variants, motivated by observed enrichment of our phenotypes for regulatory genomic regions, we computed cell type-specific enrichment for our fine-mapped GWAS SNPs on the basis of high-resolution accessible chromatin sites drawn from human primary motor cortex (M1) (27) and cerebral organoid data (28) using g-chromVAR (see Technical Workflow in Fig S9). To quantify enrichment, we computed the accessibility deviations as the expected number of feature counts per peak per cell type,

weighted by the fine-mapped variant posterior probabilities. This revealed 11 significantly positively enriched cell type-phenotype pairs after Bonferroni correction ($z>2.8$, $p<0.0025$) (Fig.5A), including enrichment of the motor-premotor region for accessible chromatin sites in oligodendrocyte precursor cells (OPCs). This result is particularly compelling given that OPCs give rise to mature oligodendrocytes which in turn myelinate axons in the central nervous system, and motor cortex is known to be a region rich in intracortical myelin content (29). For control analyses, no significant enrichment was found for metabolic traits, suggesting this approach is specific to cortical phenotypes. This approach is further supported by the consistent finding of the significant Alzheimer's-microglia pair (30).

For each significant M1 cell type-phenotype pair from Fig.5A, we identified putative causal genes from a locus' genomic position relative to its gene targets and chromatin co-accessibility relationships (i.e. both the genomic locus and its gene target were simultaneously accessible). From the initial 25 target genes, 5 distal and 2 proximal genes remained (Fig.5B) after filtering out genes with weak evidence of gene expression in the corresponding cell type (Fig S10; Table S21).

We applied the same mapping approach to pleiotropic SNPs and found 3 SNPs that overlapped with the M1 accessible chromatin peaks (Fig.5, Table S22). Noteworthy, rs2696555, a SNP in the 17q21.31 inversion region, was associated with increases in orbitofrontal area and ventral frontal thickness and mapped to the promoter region of *GRN*, a granulin precursor that helps preserve neuronal survival, axonal outgrowth and neuronal integrity through its impact on inflammatory processes in the brain (31). This SNP was also mapped at a distal putative enhancer site of *FZD2,* which encodes a Frizzled receptor within the *WNT*/beta-catenin pathway and expressed in cortical progenitor cells of the dorsal and ventral telencephalon of the developing brain (32). A schematic of how this single variant could influence area and thickness is depicted in Fig.5C.

Discussion

This study advances understanding of the genetic architecture underlying the organization of the cerebral cortex and uniquely human traits. Our genetically-informed atlases enhanced discovery of significant loci compared to previous cortical GWAS with traditional non-genetic atlases (3, 6). The improved discovery is likely aided by the fact that our atlases conform to genetic cortical patterning (4, 5), thereby increasing discoverability and heritability, while also having lower polygenicity.

Making use of two large cohorts of adults and children, we found that many genetic variants in our findings pinpoint genetic mechanisms influencing cortical patterning of the human brain in early development. Our data, particularly findings with *COUP-TF1,* support the protomap hypothesis whereby genes hold spatial and temporal instructions to initiate a cortical map by graded signaling from patterning centers in early development (1, 2). Our results are consistent with reports of loss of *COUP-TF1* function leading to expansion of frontal motor areas at the expense of posterior sensory areas in the rodent brain (1), which is intriguing given the challenges in defining rodent vs. human-specific developmental mechanisms. These variants are promising candidates for future functional experiments.

We also uncovered latent factors describing our area phenotypes, suggesting genetic effects related to inversion polymorphisms. Recurrent inversions of genomic regions, such as 17q21.31 identified here along with 8p.23, have occurred through primate evolution and show that the inverted orientation is the ancestral state. Specifically, both 17q.21.31 and 8p.23 inversions appear to have occurred independently within the *Homo* and *Pan* lineages (33, 34). 17q21.31 inversion contains *MAPT*, a risk gene for neurodegeneration (35). The inverted (minor) allele has been associated with lower susceptibility for Parkinson's dementia but higher predisposition to developmental disorders (33).

We linked several of our findings to the *WNT*/beta-catenin pathway, which regulates cortical size by controlling whether progenitors continue to proliferate or exit the cell cycle to differentiate (36). Cell proliferation is thought to exponentially enlarge the progenitor pool and the number of cortical columns, which results in expansion of cortical surface area and gyrification. On the other hand, cortical thickness is largely determined by cell differentiation and a linear production of neurons within each cortical column (2, 36). In addition to 17q21.31, our results revealed loci linked to various cortical regions in this pathway (e.g., *WNT3*, *GSK3B*), and their combined interactive effects may be differentially involved in shaping area and thickness.

The brain is particularly vulnerable to insults (genetic and environmental) during sensitive periods of neurodevelopment, and changes during this time can have lasting impacts on the brain over the lifespan. This perspective helps situate our findings of predominantly negative selection acting on our cortical phenotypes (Fig.2), which may be linked to conserved genomic loci and those enriched for neuropsychiatric diseases (18, 19). Here we uncovered a putative causal relationship of reduced anteromedial temporal area potentially giving rise to ASD. The medial temporal lobe has been linked to abnormal connectivity in some types of ASD, and houses structures (e.g. amygdala, hippocampus) important in regulating emotion and social behaviors (37). We also found this region to be enriched for accessible chromatin sites in inhibitory neurons; thus these findings may provide clues to the long-standing theory of excitatory-inhibitory imbalance in ASD (38).

Intriguingly, the majority of our phenotypes, especially paralimbic and sensory-motor regions, exhibited enriched heritability for conserved genomic partitions (Fig.3A) including promoter regions, rather than enhancers, consistent with the idea that the former are more evolutionarily conserved (18). However, we also identified brain regions that have evolved to support human-specific behaviors, such as language and communication. Differential methylation and human-specific SNPs in association with perisylvian thickness lead us to speculate that altered morphology of the perisylvian region, and potentially also motor-premotor regions, were important in the evolution of speech articulation (39).

Altogether our results with genetically-informed atlases demonstrate that human brain arealization and regionalization largely arise from phylogenetically conserved regions and multiple neurodevelopmental programs, but that a select few regulatory features, some of which may be specific to modern-day humans, have had widespread downstream effects on brain morphology and may have given rise to human-specific traits and diseases.

Supplementary Material

Refer to Web version on PubMed Central for supplementary material.

Acknowledgments:

The authors would like to thank the research participants and staff involved in data collection of the UK Biobank and Adolescent Brain Cognitive Development (ABCD) Study. The ABCD Study is a multisite, longitudinal study designed to recruit more than 10,000 children ages 9–10 and follow them over 10 years into early adulthood. The ABCD Study is supported by the National Institutes of Health and additional federal partners under award numbers U01DA041048, U01DA050989, U01DA051016, U01DA041022, U01DA051018, U01DA051037, U01DA050987, U01DA041174, U01DA041106, U01DA041117, U01DA041028, U01DA041134, U01DA050988, U01DA051039, U01DA041156, U01DA041025, U01DA041120, U01DA051038, U01DA041148, U01DA041093, U01DA041089, U24DA041123, U24DA041147. A full list of supporters is available at https://abcdstudy.org/federal-partners.html. A listing of participating sites and a complete listing of the study investigators can be found at https://abcdstudy.org/Consortium_Members.pdf. ABCD consortium investigators designed and implemented the study and/or provided data but did not all necessarily participate in analysis or writing of this report. This manuscript reflects the views of the authors and may not reflect the opinions or views of the NIH or ABCD consortium investigators.

Funding:

This research was supported by the National Institutes of Health under R01MH118281, R56AG061163, R01MH122688, R01AG050595, and R01AG022381. C.M. is supported by the Canadian Institutes of Health Research (CIHR), Fonds de Recherche du Quebec-Sante (FRQS) and the Kavli Institute for Brain and Mind (KIBM). P.M.V. and J.Y. acknowledge funding from the National Health and Medical Research Council (1113400) and the Australian Research Council (FT180100186 and FL180100072). J.Y. is supported by the Westlake Education Foundation. DvdM is supported by Research Council of Norway (project #276082). OAA is funded by the Research Council of Norway (*283798. 273291.* 248778, 223273), KG Jebsen Stiftelsen.

Data and materials availability:

The individual-level raw data used in this study can be obtained from two accessible data resources, UK Biobank (https://www.ukbiobank.ac.uk/) and ABCD Study (https://abcdstudy.org). ABCD Study data were processed from the raw structural imaging data held in the NIMH Data Archive (NDA). The ABCD data repository grows and changes over time. The ABCD data used in this report came from ABCD Collection Release 2.0.1 (40). Data access details can be found on the NDA website (https://nda.nih.gov/abcd/request-access). GWAS summary statistics are accessible in an NDA Study (DOI is 10.15154/1523026) (41). We made use of publicly available software and tools. The analysis code is available in the Bio-protocol.

References and notes:

1. Molnár Z, Clowry GJ, Šestan N, et al. : New insights into the development of the human cerebral cortex. J Anat 2019; 235:432–451 [PubMed: 31373394]
2. Rakic P: Evolution of the neocortex: a perspective from developmental biology. Nat Rev Neurosci 2009; 10:724–735 [PubMed: 19763105]
3. Grasby KL, Jahanshad N, Painter JN, et al. : The genetic architecture of the human cerebral cortex. Science 2020; 367
4. Chen C-H, Gutierrez ED, Thompson W, et al. : Hierarchical genetic organization of human cortical surface area. Science 2012; 335:1634–1636 [PubMed: 22461613]
5. Chen C-H, Fiecas M, Gutiérrez ED, et al. : Genetic topography of brain morphology. Proc Natl Acad Sci U S A 2013; 110:17089–17094

6. van der Meer D, Frei O, Kaufmann T, et al. : Quantifying the Polygenic Architecture of the Human Cerebral Cortex: Extensive Genetic Overlap between Cortical Thickness and Surface Area. Cereb Cortex 2020; 30:5597–5603 [PubMed: 32483632]
7. Jiang L, Zheng Z, Qi T, et al. : A resource-efficient tool for mixed model association analysis of large-scale data. Nat Genet 2019; 51:1749–1755 [PubMed: 31768069]
8. Purcell S, Neale B, Todd-Brown K, et al. : PLINK: a tool set for whole-genome association and population-based linkage analyses. Am J Hum Genet 2007; 81:559–575 [PubMed: 17701901]
9. Watanabe K, Taskesen E, van Bochoven A, et al. : Functional mapping and annotation of genetic associations with FUMA. Nat Commun 2017; 8:1826 [PubMed: 29184056]
10. Yang J, Lee SH, Goddard ME, et al. : GCTA: a tool for genome-wide complex trait analysis. Am J Hum Genet 2011; 88:76–82 [PubMed: 21167468]
11. Gogarten SM, Sofer T, Chen H, et al. : Genetic association testing using the GENESIS R/Bioconductor package. Bioinformatics 2019; 35:5346–5348 [PubMed: 31329242]
12. See Supplementary Material
13. Yang J, Ferreira T, Morris AP, et al. : Conditional and joint multiple-SNP analysis of GWAS summary statistics identifies additional variants influencing complex traits. Nat Genet 2012; 44:369–75, S1–3 [PubMed: 22426310]
14. Zhu Z, Zheng Z, Zhang F, et al. : Causal associations between risk factors and common diseases inferred from GWAS summary data. Nat Commun 2018; 9:224 [PubMed: 29335400]
15. Zaitlen N, Kraft P, Patterson N, et al. : Using extended genealogy to estimate components of heritability for 23 quantitative and dichotomous traits. PLoS Genet 2013; 9:e1003520
16. Zeng J, de Vlaming R, Wu Y, et al. : Signatures of negative selection in the genetic architecture of human complex traits. Nat Genet 2018; 50:746–753 [PubMed: 29662166]
17. Matoba N, Love MI, Stein JL: Evaluating brain structure traits as endophenotypes using polygenicity and discoverability. Hum Brain Mapp 2020
18. Hujoel MLA, Gazal S, Hormozdiari F, et al. : Disease Heritability Enrichment of Regulatory Elements Is Concentrated in Elements with Ancient Sequence Age and Conserved Function across Species. Am J Hum Genet 2019; 104:611–624 [PubMed: 30905396]
19. Gazal S, Loh P-R, Finucane HK, et al. : Functional architecture of low-frequency variants highlights strength of negative selection across coding and non-coding annotations. Nat Genet 2018; 50:1600–1607 [PubMed: 30297966]
20. Trynka G, Raychaudhuri S: Using chromatin marks to interpret and localize genetic associations to complex human traits and diseases. Curr Opin Genet Dev 2013; 23:635–641 [PubMed: 24287333]
21. Gokhman D, Lavi E, Prüfer K, et al. : Reconstructing the DNA methylation maps of the Neandertal and the Denisovan. Science 2014; 344:523–527 [PubMed: 24786081]
22. Grotzinger AD, Rhemtulla M, de Vlaming R, et al. : Genomic structural equation modelling provides insights into the multivariate genetic architecture of complex traits. Nat Hum Behav 2019; 3:513–525 [PubMed: 30962613]
23. Hogstrom LJ, Westlye LT, Walhovd KB, et al. : The structure of the cerebral cortex across adult life: age-related patterns of surface area, thickness, and gyrification. Cereb Cortex 2013; 23:2521–2530 [PubMed: 22892423]
24. Kwon T-J, Cho H-J, Kim U-K, et al. : Methionine sulfoxide reductase B3 deficiency causes hearing loss due to stereocilia degeneration and apoptotic cell death in cochlear hair cells. Hum Mol Genet 2014; 23:1591–1601 [PubMed: 24191262]
25. Minniti AN, Arrazola MS, Bravo-Zehnder M, et al. : The Protein Oxidation Repair Enzyme Methionine Sulfoxide Reductase A Modulates Aβ Aggregation and Toxicity In Vivo. Antioxidants & Redox Signaling 2015; 22:48–62 [PubMed: 24988428]
26. Lo M-T, Hinds DA, Tung JY, et al. : Genome-wide analyses for personality traits identify six genomic loci and show correlations with psychiatric disorders. Nat Genet 2017; 49:152–156. [PubMed: 27918536]
27. Bakken TE, Jorstad NL, Hu Q, et al. : Evolution of cellular diversity in primary motor cortex of human, marmoset monkey, and mouse. bioRxiv 2020

28. Kanton S, Boyle MJ, He Z, et al. : Organoid single-cell genomic atlas uncovers humanspecific features of brain development. Nature 2019; 574:418–422 [PubMed: 31619793]
29. Glasser MF, Van Essen DC: Mapping human cortical areas in vivo based on myelin content as revealed by T1- and T2-weighted MRI. J Neurosci 2011; 31:11597–11616
30. Lake BB, Chen S, Sos BC, et al. : Integrative single-cell analysis of transcriptional and epigenetic states in the human adult brain. Nat Biotechnol 2018; 36:70–80 [PubMed: 29227469]
31. Gao X, Joselin AP, Wang L, et al. : Progranulin promotes neurite outgrowth and neuronal differentiation by regulating GSK-3β. Protein Cell 2010; 1:552–562 [PubMed: 21204008]
32. Harrison-Uy SJ, Pleasure SJ: Wnt signaling and forebrain development. Cold Spring Harb Perspect Biol 2012; 4:a008094
33. Zody MC, Jiang Z, Fung H-C, et al. : Evolutionary toggling of the MAPT 17q21.31 inversion region. Nat Genet 2008; 40:1076–1083 [PubMed: 19165922]
34. Salm MPA, Horswell SD, Hutchison CE, et al. : The origin, global distribution, and functional impact of the human 8p23 inversion polymorphism. Genome Res 2012; 22:1144–1153 [PubMed: 22399572]
35. Strang KH, Golde TE, Giasson BI: MAPT mutations, tauopathy, and mechanisms of neurodegeneration. Lab Invest 2019; 99:912–928 [PubMed: 30742061]
36. Chenn A, Walsh CA: Regulation of cerebral cortical size by control of cell cycle exit in neural precursors. Science 2002; 297:365–369 [PubMed: 12130776]
37. Rane P, Cochran D, Hodge SM, et al. : Connectivity in Autism: A Review of MRI Connectivity Studies. Harv Rev Psychiatry 2015; 23:223–244 [PubMed: 26146755]
38. Cellot G, Cherubini E: GABAergic signaling as therapeutic target for autism spectrum disorders. Front Pediatr 2014; 2:70 [PubMed: 25072038]
39. Gokhman D, Nissim-Rafinia M, Agranat-Tamir L, et al. : Differential DNA methylation of vocal and facial anatomy genes in modern humans. Nat Commun 2020; 11:1189 [PubMed: 32132541]
40. DOI: 10.15154/1504041
41. DOI: 10.15154/1523026

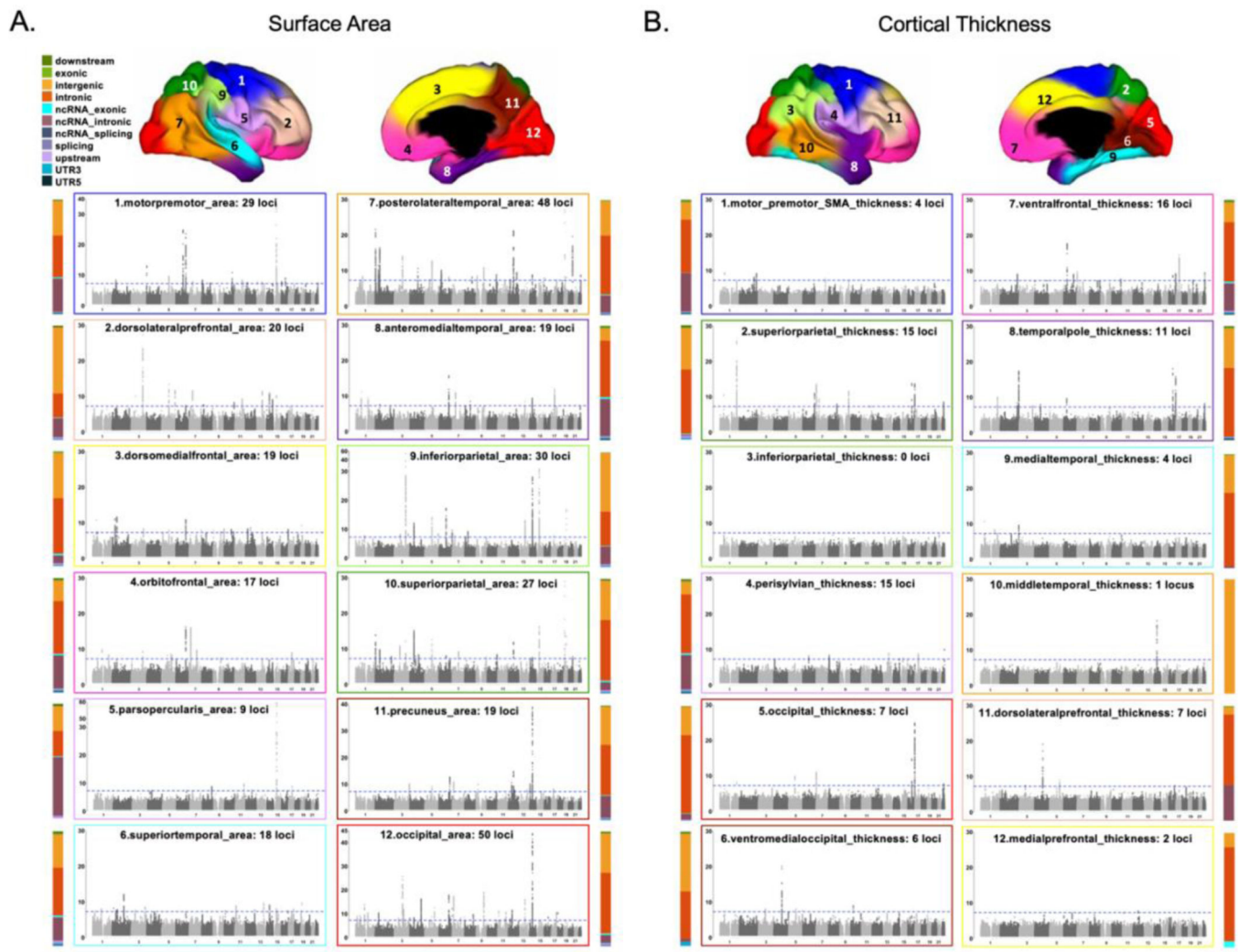

Fig.1. Manhattan plots of genetic variants underlying cortical thickness and area.

Results are shown separately for surface area (Panel A) and cortical thickness (Panel B). Numbers on brain atlases represent each brain region. Plots are color-coded for brain atlas region. Number of significant genetic loci are listed in Manhattan subplot titles, with the horizontal dotted line denoting genome-wide significance. Vertical bar charts show breakdown of genomic position of SNPs, with corresponding legend at top of Panel A.

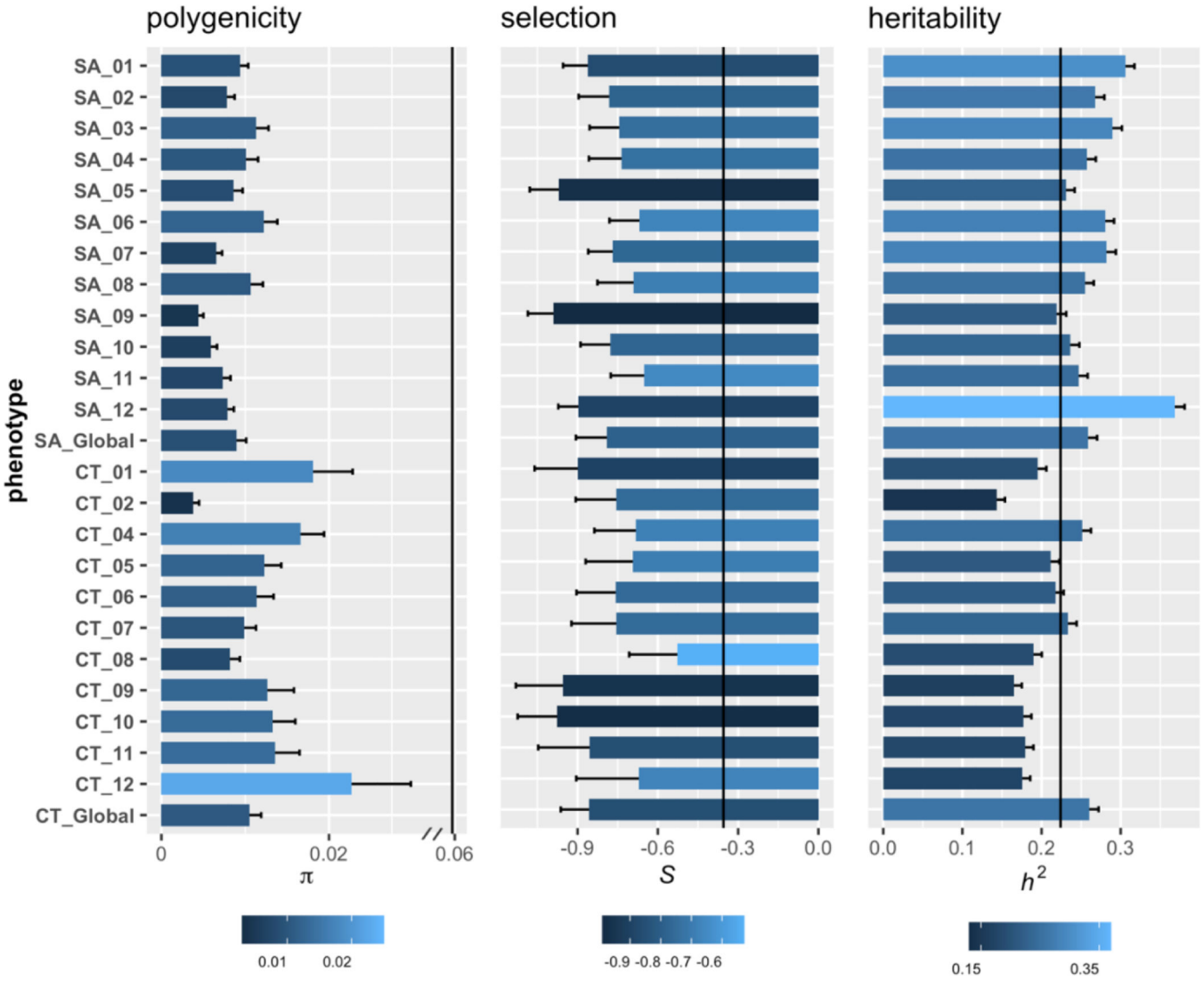

Fig.2. Genetic architecture of the cortex.

Cortical phenotypes generally have low polygenicity, medium/high heritability and are under strong negative selection. Vertical black lines on each plot are average reference lines for relevant estimates of commonly studied traits taken from (16). Numbering of regions follows labels in Fig.1.

Abbreviations: SA: Surface Area. CT: Cortical Thickness. π: polygenicity. S: selection. h^2: heritability.

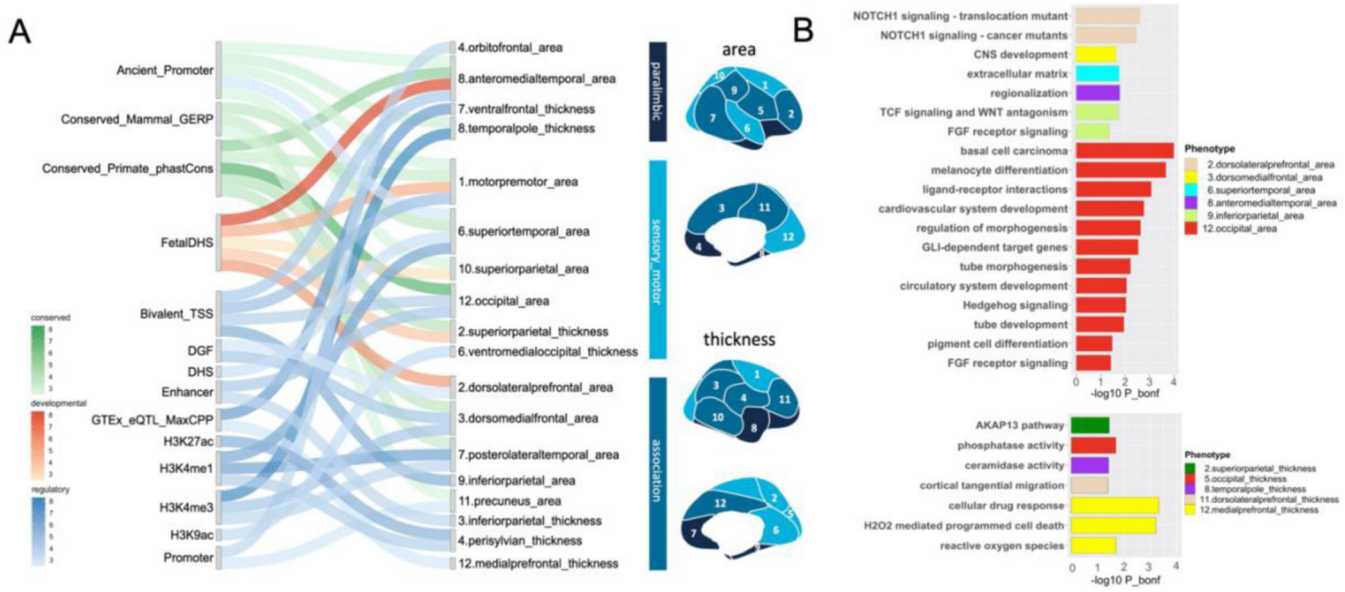

Fig.3. Partitioned heritability and Gene Ontology (GO) enrichment.

Panel A. Heritability of cortical phenotypes are significantly enriched for conserved, developmental, and regulatory annotations. The river plot depicts mapping between significant annotations (18) and cortical phenotypes. Color-coding of river plot is based on -log10 enrichment p-values.

Panel B. Significantly enriched GO terms from MAGMA gene-set analysis for surface area (top) and cortical thickness (bottom).

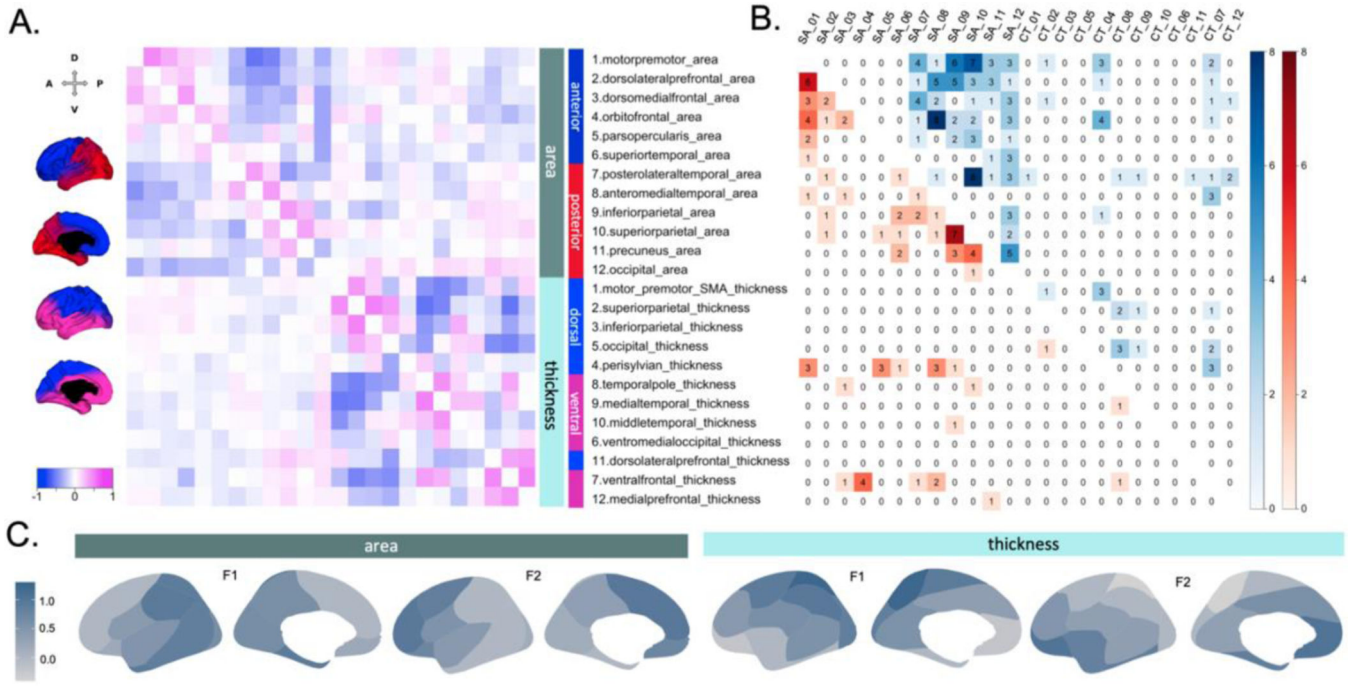

Fig. 4. Three-dimensional genetic characterization of cortex.

Panel A. Phenotypic and genotypic correlations between 24 regions, ordered by hierarchical clustering that shows A-P divisions for area, and D-V divisions for thickness. Phenotypic correlations are in bottom left triangle and genetic correlations in upper right.

Panel B. Pleiotropic SNP counts for each pair of regions, using the same ordering as Panel A. Agonistic or same direction of effects are in lower red triangle; antagonistic or opposing effects are in upper blue triangle.

Panel C: Brain maps of standardized effects of each latent factor (F1 and F2) derived from genomic SEM on each brain region. Detailed statistics are in Fig.S7.

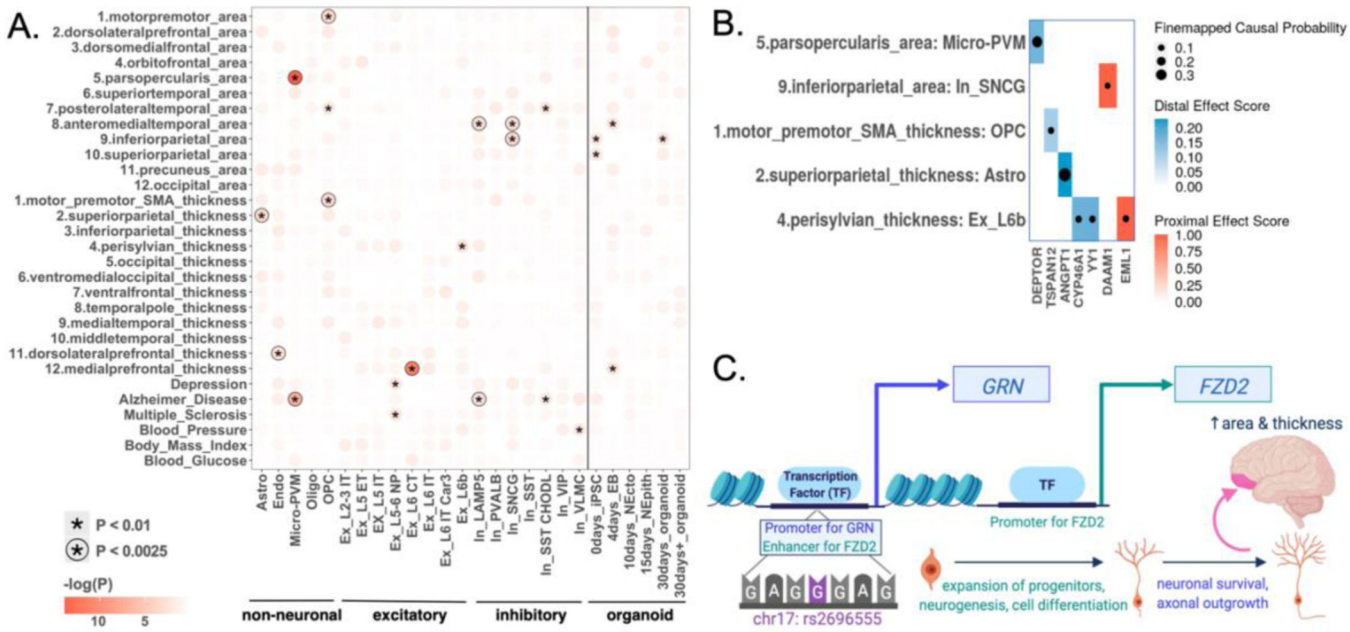

Fig.5. Enrichment of cell type-specific accessible chromatin sites and fine-mapping to regulatory regions of genes.

Panel A. Heatmap of enrichment for cortical phenotypes and cell type-specific accessible chromatin peaks. Phenotypes also include 3 metabolic (blood glucose, body mass index, blood pressure) and 3 cortical-related (multiple sclerosis, Alzheimer's Disease, depression) controls. Vertical black line differentiates M1 cell types (left) from organoid developmental stages (right). Significant values are based on the bias-corrected enrichment statistic from g-chromVAR (12). Panel B. Mapped genes and the regulatory region (blue=enhancer; red=promoter) of the causal SNPs carried forward by positively enriched M1 cell type-cortical phenotype pairs ($z>2.36$, $p<0.01$). Size of dot reflects probability of SNP being causal. Colors represent peak to gene coaccessibilities, where a score of 1 reflects a peak being in the gene's promoter region. Panel C. A selected pleiotropic SNP (rs2696555) influencing both orbitofrontal area and ventral frontal thickness, mapped to target genes based on co-accessibility with M1. Cell types are outlined in Table S23.